

Digital response with femtosecond resolution in an optical AND gate

G. R. Collecutt and P. D. Drummond^a

^a*Department of Physics, The University of Queensland, QLD 4072, AUSTRALIA.
Ph: +61 7 3365 3405, Fax: +61 7 3365 1242, email: collecug@physics.uq.edu.au*

Abstract

We present a numerical simulation of an all-optical AND logic gate utilising soliton formation in a planar waveguide with a parametric nonlinearity. We investigate switching performance as a function of input logic simultaneity and internal geometry. A highly digital response in transmitted pulse energy is observed, with femtosecond time discrimination.

PACS codes: 42.65.P 42.65.T 42.79.T

Keywords: parametric, soliton, nonlinear, optical, logic.

For around three decades now the all-optical processor has proved elusive, with mixed opinions as to how it may be achieved [1]. The growth and performance of silicon based electronics has truly exceeded all expectations, but as a direct consequence of this performance we have a rapidly growing global information network which is continually pushing networking technology to its limits. Fibre optics is very successfully solving the need for simple information propagation, but up until recently optical signals had to be continually received and resent for two purposes: amplification and routing. This process of receiving signals and re-sending them is expensive and slow in comparison to the huge bandwidth available within an optical fibre, and is one of the primary bottle-necks in an optical information network. Now that the erbium doped fibre laser is proving itself as a practical and effective optical amplifier, all that remains is to be able to route information while it remains in optical form. Signal routing, multiplexing, demultiplexing, and regeneration are present applications for all-optical logic switching.

In this paper we describe the theory of a parametric type II soliton based optical AND gate. In particular, we find the switching performance to be a highly digital function of pulse timing. The optical AND gate can operate with

a pulse FWHM as short as 30fs, and it shows digital response with a resolution of order 1fs, provided Raman scattering and higher order dispersion can be neglected. A closely related type I device has already been experimentally demonstrated with 100fs pulse duration [2].

To illustrate one of the main problems involved with all optical switching, consider first the requirements for the operation of an AND logic gate. In order to obtain a logic true output, each of the logic inputs must know about the presence of the other. This is essentially a nonlinear process. However, light in the majority of dielectrics is the solution to the linear Maxwell equations, and thus does not interact with other light. A dielectric with nonlinear response is needed. In recent years there have been considerable advances in the theory and manufacture of such nonlinear optical media, which now opens up a new and exciting range of possibilities for all optical logic circuits. One such possibility is the implementation of an all-optical AND gate as proposed by Drummond et. al. [3] and re-illustrated in Figure 1.

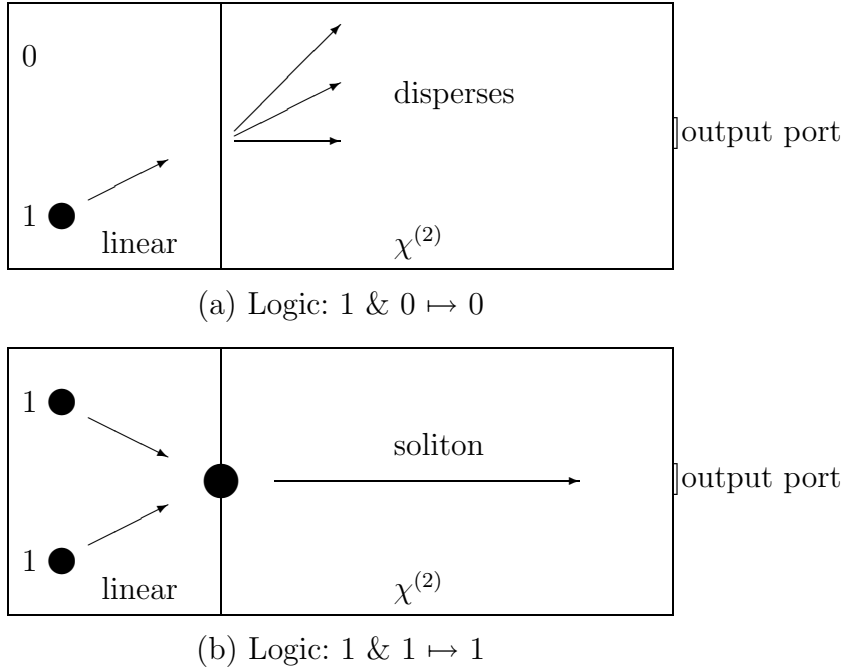


Fig. 1. Schematic of proposed AND gate implementation.

In this method two simultaneous dispersive input pulses are collided at the boundary of a planar parametric waveguide to form a 2+1D spatiotemporal soliton, which propagates stably towards the output port. If only one input pulse is present then it simply disperses with little or no energy reaching the output. Clearly if there are no pulses present then there will be no output. Hence, AND gate logic is achieved. The basic entity used is the 2+1D parametric spatiotemporal soliton, which was proposed in 1997 by Malomed et. al. [4], and was experimentally observed last year by Liu et. al. [5]. The two main requirements are anomalous dispersion and (near) group velocity matching

at the fundamental and second harmonic frequencies. We emphasise that the method uses nonlinear spatiotemporal soliton *formation* [6] as the key element. In this respect it is completely distinct from other proposals [7,8] for optical logic gates based on soliton collisions or spatial soliton interactions.

There are two different methods by which the input pulses can interact: type I interaction, where the pulses are of the same polarisation; or type II interaction, where the pulses are of orthogonal polarisations. For the purpose of logic switching it would be ideal for all input and output pulses to be identical, i.e. the same carrier frequency, polarisation, and similar shape and intensity. The difficulty with completely degenerate pulses, as pointed out by Assanto [8] and also by Drummond et. al [3], is that the interaction would be phase sensitive, and precise optical phasing is difficult to control. As a result, if we are to avoid controlling precise pulse phases, we must resort to making the pulses nondegenerate either in frequency or polarisation. Further, if we are to link serially a number of these optical AND gates, we will need to be able to convert one type of logic bit to the other. This is more easily done in polarisation than in frequency, thus favouring type II interaction. Equations 1 – 3 describe the 2+1D non-degenerate (type II) parametric interaction in dimensionless coordinates [3].

$$\frac{\partial \phi_1}{\partial \xi} = i \left[\left(\frac{\partial^2}{\partial \tau^2} + \frac{\partial^2}{\partial \zeta^2} + i\nu_{gvm} \frac{\partial}{\partial \tau} + i\Gamma(\tau, \zeta) - 1 \right) \phi_1 + \phi_2^* \phi_3 \right]; \quad (1)$$

$$\frac{\partial \phi_2}{\partial \xi} = i \left[\left(\frac{\partial^2}{\partial \tau^2} + \frac{\partial^2}{\partial \zeta^2} - i\nu_{gvm} \frac{\partial}{\partial \tau} + i\Gamma(\tau, \zeta) - 1 \right) \phi_2 + \phi_1^* \phi_3 \right]; \quad (2)$$

$$\frac{\partial \phi_3}{\partial \xi} = i \left[\left(\frac{1}{\sigma} \frac{\partial^2}{\partial \tau^2} + \frac{1}{2} \frac{\partial^2}{\partial \zeta^2} + i\Gamma(\tau, \zeta) - \gamma \right) \phi_3 + \phi_1 \phi_2 \right] . \quad (3)$$

Here σ is the ratio of dispersion between fundamental and second harmonic frequencies, and γ is a phase velocity mismatch parameter for the second harmonic field. For the results presented, σ was set to 2 (yielding $\tau - \zeta$ symmetry) and γ was set to 1. The group velocities of the fundamental fields are assumed to symmetrically straddle the group velocity of the second harmonic field; the reciprocals of the velocities differing by $\pm\nu_{gvm}$. $\Gamma(\tau, \zeta)$ is a damping field applied in the numerical simulations to absorb scattered radiation at the lattice boundaries. The theory here is somewhat idealised, in that these equations neglect higher order dispersion, Raman scattering, second harmonic group velocity mismatch, and spatial walk-off effects, as well as any possible effects due to nonlinear dispersion. The variable transformation is given by:

$$\phi_i = \frac{\Phi_i}{\Phi_0}; \quad \xi = \frac{z}{z_0}; \quad \zeta = \frac{y}{y_0}; \quad \tau = \frac{t - z/v_{g3}}{t_0}; \quad \nu_{gvm} = \frac{z_0}{ct_0} \frac{n_{g2} - n_{g1}}{2} , \quad (4)$$

where $|\Phi_0|^2$ is a reference photon flux, z is the direction of propagation, y is the transverse coordinate, and t is time. Equations 5 and 6 (derived from [10]) define the scalars y_0 , t_0 , and Φ_0 :

$$y_0 = \sqrt{\frac{z_0}{2k_0}}; \quad t_0 = \sqrt{\frac{z_0\beta_2}{2}}; \quad \Phi_0 = \frac{1}{\chi z_0}, \quad (5)$$

$$\chi = \chi^{(2)} \sqrt{\frac{\hbar k_0^3}{\epsilon_0 n^3}} \int u^{(1)}(u^{(2)})^* u^{(1)} dx, \quad (6)$$

where k_0 is the fundamental wave number in free space, β_2 is the second dispersion, n is the refractive index at the fundamental wavelength, and χ is derived from the $\chi^{(2)}$ nonlinearity and mode shape integral.

To investigate this process of soliton formation, numerical simulations of type I and type II interactions have been performed using a central step partial difference integration method [9] on a two dimensional lattice. Figures 2 and 3 display the results for type II interaction: Figure 2 being for the case of only one input pulse, and Figure 3 for the case of simultaneous input pulses. Here we are plotting the transverse cross-section (through $\tau = 0$) of total power density ($|\phi_1|^2 + |\phi_2|^2 + 2|\phi_3|^2$) as a function of propagation distance.

Due to reasons that will be covered shortly, we require nonlinear evolution of the order of 10 units of z_0 in order to effect the switch. If this is required within an available length of $\chi^{(2)}$ media of say 50mm, then $z_0 = 5\text{mm}$. Assuming (very approximately) a square mode profile then the mode shape integral will evaluate to $1/\sqrt{d}$ where d is the depth of the planar guide. Taking typical values for nonlinearity, dispersion, and fundamental wavelength of $\chi^{(2)} = 10\text{pm/V}$, $\beta_2 = 25\text{ps}^2/\text{km}$, and $\lambda = 1.5\mu\text{m}$ respectively, we obtain $y_0 = 24.43\mu\text{m}$ and $t_0 = 7.91\text{fs}$. Finally with a waveguide depth of $2\mu\text{m}$ we get $\Phi_0 = 1.58 \times 10^{12}(\text{photons/m/s})^{\frac{1}{2}}$.

Figures 2 and 3 were originally calculated in dimensionless coordinates, in which the propagation was for 10 units of z_0 with the GVM between the fundamental fields set to zero. The initial pulses used were radially symmetric Gaussians ($r^2 = \tau^2 + \zeta^2$) with an amplitude of $\phi_0 = 7.5$ and radius $r_0 = 2$. Their initial transverse velocities were ± 1 unit of y_0 for every unit of z_0 , and for Figure 3 their centres were still 0.40 units of y_0 apart and converging when they launched. The pulses were also simultaneous, i.e. both centered on $\tau = 0$. The second harmonic field (ϕ_3) was initialised to zero. Using the above scaling the input pulses were then $98\mu\text{m}$ in width and 31.6fs in duration (FWHM both cases). This yields a total energy for each input pulse of 22.6pJ . Hence for Figure 3 the pulses were converging at an included angle of 0.56° and their centres were still $9.8\mu\text{m}$ apart at the start of the nonlinear medium. The software package developed for these simulations is available at [11] and the

input scripts for the simulations depicted in Figures 2 and 3 are available at [12].

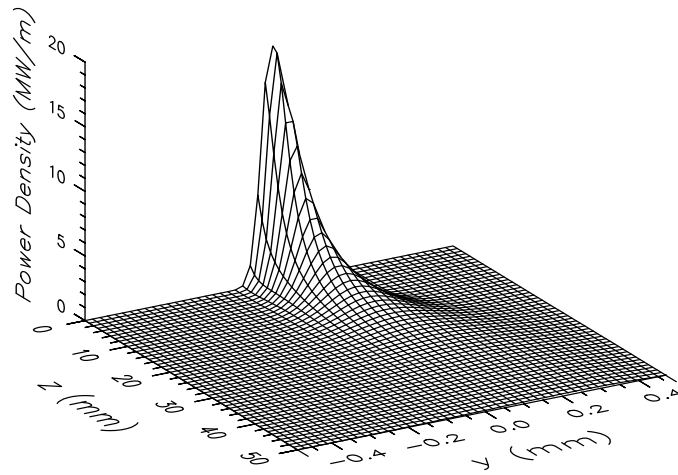


Fig. 2. Single pulse input.

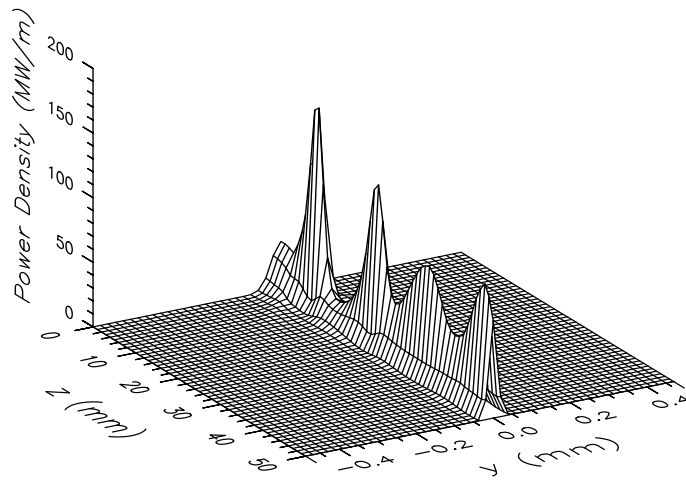


Fig. 3. Soliton formation process.

As can be seen in Figure 3 a breathing soliton forms when both input pulses are present, whereas in Figure 2 the input pulse energy of a single pulse is seen to disperse. It is reasonable to use either of the fundamental fields or

even the second harmonic field for the switch output, but not all three. We have chosen here to plot total power density because it is the more revealing moment with regard to understanding the dynamics of the interaction, not because it defines the output of the switch.

From our studies we have found several interesting points of behaviour. Firstly, it is interesting to note that to form a soliton the pulses must be overlapped as they enter the nonlinear medium. We have been unable to form a soliton with input pulses that are initially separate.

Secondly, it is possible to repeat the above simulations for the case of completely degenerate pulses simply by superposing both inputs in one fundamental field and using the appropriate equations for frequency degenerate type I interaction. The pulses must initially be separate in order to superpose them, and a length of linear propagation is then necessary to overlap the pulses. In the case where the input pulses are in phase we find soliton formation occurs in much the same way as for the type II case, but when they are anti-phased we find the energy scatters after collision, thus confirming that this is a phase dependent process [8,3].

Thirdly, we find the process of soliton formation is sensitive to exactly how the input pulses are overlapped in transverse dimension and in time. Figure 4 shows the transmitted energy to the output port as a function of time and transverse separation. The width of the output port was the same as that of the input pulses: 4 units of y_0 , or $98\mu\text{m}$. The notation here is that negative transverse separation indicates that the pulses are still converging at launch. The response is symmetric in time separation as ν_{gvm} was maintained at zero.

There are four key regions in this figure. Firstly, a relatively flat plateau can be seen in the central region of the figure. This is where one crisp soliton is formed and propagates stably to the output port; it represents logic 1 output. Secondly note the steep wall in the region of $-26\mu\text{m}$ transverse separation and zero time separation. This is where the soliton formation process becomes unstable and the initial packet of energy breaks into two solitons, which then repel each other. When the time separation is zero they repel each other in the transverse direction, thus they straddle the output port at the end of the switch and no energy is transmitted. However, with the right ratio of initial transverse separation and time separation we find that the break up is purely along the longitudinal (time) coordinate. This results in both solitons arriving at the output port one after the other – their combined energy being visible in Figure 4 as the “arms” leading away from the plateau; the third region. This behaviour is highly undesirable but may be easily avoided: the initial transverse separation of the pulses is determined by the geometry of the lead in channels in the switch, and as such is a manufacturing tolerance issue. If the switch can be manufactured so that this separation is within an appropriate

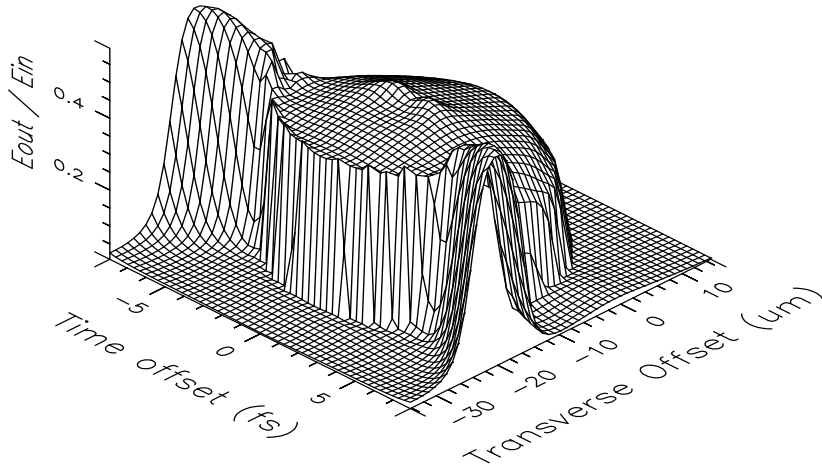


Fig. 4. Transmitted energy for the type II interaction with a relative convergence angle of 0.56° .

tolerance band (say $-8\mu\text{m} \pm 2\mu\text{m}$ for this set up) then all should be well. We will see a response which is primarily a function of time separation. This is shown in Figure 5 for $-9.8\mu\text{m}$ transverse separation, and brings us to the fourth and final region of interest – the plateau wall in this vicinity.

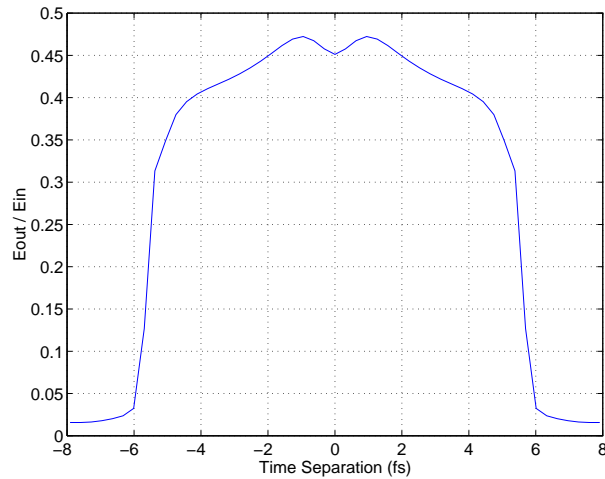


Fig. 5. Transmitted energy vs time separation for transverse separation = $-9.8\mu\text{m}$.

Here we see what appears to be a fairly digital response to the time separation of the input pulses. In fact, the switch appears to be capable of rising from near zero response to near maximum response for about a 1fs change in input pulse timing. The effect is not quite as digital as the wall at the front of Figure 4 (earlier referred to as the second region), because here the breakup

mechanism forms three solitons: two flying away with both transverse velocity and longitudinal velocity, and the third remaining central. In order that the response be as digital as possible, we require that the any soliton break-ups be fully effected before the soliton reaches the output port. This is why we required a nonlinear propagation of 10 units of z_0 , as stated earlier.

Finally, we must consider the reality that there will be some degree of GVM between the fundamental fields. This has been investigated using the base case (as used for Figure 3) and varying the GVM from $\nu_{gvm} = 0$ to $\nu_{gvm} = 2$. The results are shown in Figure 6, in which the abscissa is now shown in units of $|n_{g2} - n_{g1}|$. Here we can see that a mismatch of up to 0.0005 in $|n_{g2} - n_{g1}|$ has little effect, but beyond this the soliton fails to form.

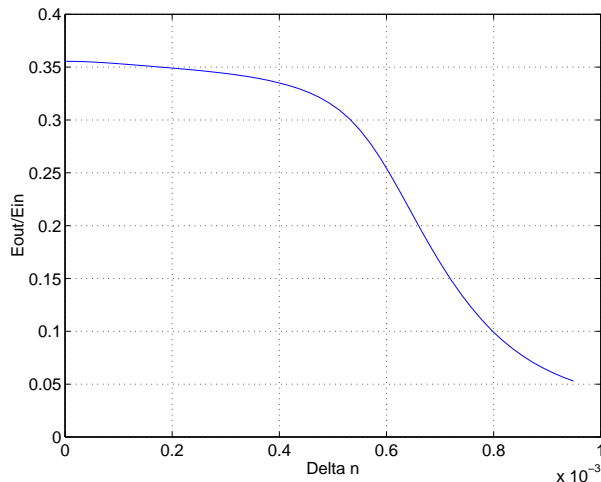


Fig. 6. Transmitted energy vs FF GVM

In conclusion we have shown that it is possible to achieve an all-optical AND gate using spatiotemporal soliton formation in a parametric medium. The interaction between fully degenerate input pulses was studied briefly and proved to be highly sensitive to the relative phase difference between the input pulses. The interaction between input pulses that were nondegenerate in polarisation was studied in detail and was found to be complex in nature. In particular a highly digital response with regard to relative pulse timing was found. Our estimates indicate that pulse durations as short as 30fs are feasible, with pulse energies in the picjoule range and digital timing discrimination as short as 1fs, in this idealised model.

References

- [1] T. E. Bell, "Optical computing: a field in flux", IEEE Spectrum **23**, 34-57 (1986).
- [2] X. Liu, L. J. Qian, and F. W. Wise, "Noncollinear Generation of optical

spatiotemporal solitons and application to ultrafast digital logic”, Accepted by Phys. Rev. E, awaiting printing (2000).

- [3] P. D. Drummond, K. V. Kheruntsyan, and H. He, “Novel solitons in parametric amplifiers and atom lasers”, J. Opt. B **1**, 387-395 (1999).
- [4] B. A. Malomed, P. D. Drummond, H. He, A. Berntson, D. Anderson, and M. Lisak, “Spatiotemporal solitons in multidimensional optical media with a quadratic nonlinearity” Phys. Rev. E **56**, 4725-4735 (1997).
- [5] X. Liu, L. J. Qian, and F. W. Wise, “Generation of optical spatiotemporal solitons”, Phys. Rev. Lett. **82**, 4631-4634 (1999).
- [6] P. D. Drummond, “Formation and stability of vee simultons”, Opt. Commun. **49**, 219-223 (1984).
- [7] M. N. Islam and C. E. Socolich, “Billiard-ball soliton interaction gates”, Opt. Lett. **16**, 1490-1492 (1991); G. Leo, G. Assanto, W. E. Torruellas, “Intensity-controlled interactions between vectorial spatial solitary waves in quadratic nonlinear media”, Opt. Lett. **22**, 7-9, (1997).
- [8] G. Assanto, “Transistor action through nonlinear cascading in type-II interactions”, Opt. Lett. **20**, 1595-1597 (1995).
- [9] P. D. Drummond, “Central partial difference algorithms”, Computer Phys. Commun. **29**, 211-225 (1983).
- [10] M. J. Werner and P. D. Drummond, “Pulsed quadrature-phase squeezing of solitary waves in $\chi^{(2)}$ parametric waveguides”, Phys. Rev. A **56**, 1508-1518 (1997).
- [11] The software package used to perform the simulations in Figures 2 and 3 is called *XMDS*, and is available at <http://physics.uq.edu.au/xmds>
- [12] The input scripts for the simulations in Figures 2 and 3 are available at <http://physics.uq.edu.au/xmds/scripts>